
Article:
Walton, Paul Howard orcid.org/0000-0002-1152-1480, Labourel, Aurore, Frandsen, Kristian E H et al. (17 more authors) (2020) A fungal family of lytic polysaccharide monooxygenase-like copper proteins. NATURE CHEMICAL BIOLOGY. https://doi.org/10.1038/s41589-019-0438-8. pp. 1-11. ISSN: 1552-4450

https://doi.org/10.1038/s41589-019-0438-8

Supplementary Tables.

Supplementary Table 1. Fungal X325 enzymes that have been recombinantly produced in *Pichia pastoris*.

Name	Fungi	Protein ID
*Lb*X325	*Laccaria bicolor*	XP_001874295.1
*La*X325	*Laetisaria arvalis*	MK088083
*Pa*X325	*Podospora anserina*	XP_001907559.1
*Yl*X325	*Yarrowia lipolytica*	XP_505821.1

Supplementary Table 2: Crystallographic data collection and refinement statistics.

	*La*X325 $P2_12_12_1$	*La*X325 $P4_32_12$	*La*X325 $P2_1$
Data collection			
Space group	$P2_12_12_1$	$P4_32_12$	$P2_1$
Cell dimensions			
a, *b*, *c* (Å)	84.60 , 84.64 , 127.32	74.92, 74.92, 64.39	32.94, 67.59, 68.90
α, β, γ (°)	90.000, 90.000, 90.000	90.000, 90.000, 90.000	90.000, 97.939, 90.000
Mol/ASU	4	1	2
Resolution (Å)	100 - 2.08 (2.13 – 2.08)*	60 - 2.10 (2.15 – 2.10)	68.25 -1.82 (1.87 – 1.82)
R_{meas}	0.152 (1.398)	0.087 (1.703)	0.097 (0.911)
$I / \sigma I$	12.93 (1.07)	12.25 (1.49)	11.79 (2.12)
Completeness (%)	99.6 (98.5)	99.9 (99.9)	95.1 (68.9)
Redundancy[$]	14.0 (14.3)	7.2 (7.4)	7.4 (6.3)
No. of reflections	775853 (55401)	80479 (6008)	188926 (8457)
No unique of reflections	57268 (4005)	11173 (807)	25629 (1351)
CC½ (%)	99.8 (74.4)	99.9 (80.3)	99.7 (81.6)
Refinement			
Resolution (Å)	42.35 - 2.08 (2.13 – 2.08)	48.88 - 2.10 (2.15 - 2.10)	68.24 -1.82 (1.86 – 1.82)
No. reflections	52714 (3752)	10600 (575)	24384 (1262)
R_{work} / R_{free} (%)	24.4 / 27.1 (45.1 / 49.0)	19.35/ 25.6 (34.3 / 34.1)	16.7 / 20.8 (33.9 / 32.8)
No. atoms			
Protein[§]	A: 1257, B : 1215, C : 1276, D : 1184	A: 1182	A : 1241, B : 1209
Solvent[#]	614	55	192
B-factors (Å^2)			
Protein	A: 39.1, B: 43.5 C: 43.8, D: 55.5	A: 57.6	A : 38.5 B : 40.8
Solvent	50.4	58.0	46.7
R.m.s. deviations			
PDB code	6IBI	6IBJ	6IBH

One of crystal was used for each structure.
*Values in parentheses are for highest-resolution shell.
$ Friedel pairs are treated as symmetry-equivalent reflections
§ Glycosylation (N-acetylglucosamine units) and the active site copper are included in "Protein"
# PEG, imidazole and water molecules are included under "Solvent"

Supplementary Table 3. Cu-ligand distances and geometry of coordination.

Protein	Spacegroup	mol	Equatorial ligand positions (Å)				axial positions (Å)		Cu-ligand angles (°)¤			PDB
Macromolecules			**Cu-NH_2**	**Cu-Nδ**	**Cu- Nε/(Nδ)**	**Cu-O**	**Cu-O§**	**Cu-H_2O_{ax}**	Θ1	Θ2	Θ3	
*La*X325	$P2_12_12_1$	A	2.04	2.03	2.06	2.00	(2.88)	2.51	92.4	88.5	169.6	6IBI
*La*X325	$P2_12_12_1$	B	2.03	2.06	2.00	2.02	(2.99)	N/A	91.3	90.4	176.1	6IBI
*La*X325	$P2_12_12_1$	C	2.08	2.02	2.03	2.07	(2.97)	2.35	90.4	88.3	178.7	6IBI
*La*X325	$P2_12_12_1$	D	2.02	2.01	2.05	2.02	(3.07)	N/A	92.9	88.8	178.3	6IBI
*La*X325	$P4_32_12$	A	2.02	2.04	2.03	1.98	(3.00)	N/A	91.7	86.0	175.4	6IBJ
*La*X325	$P2_1$	A	2.04	2.03	2.03	2.09	(2.86)	2.65	94.5	84.7	177.8	6IBH
*La*X325	$P2_1$	B	2.05	2.05	2.04	2.08	(2.82)	2.28	94.6	84.5	176.5	6IBH
Mean and standard deviations			2.04 ±0.02	2.03 ±0.02	2.03 ±0.02	2.04 ±0.04	2.94 ±0.09	2.45 ±0.17	92.5 ±1.6	87.1 ±2.4	176.1 ±3.1	
*Td*AA15§	$P22_12_1$	A	2.16	2.00	1.99	N/A	2.56	N/A	96.0	94.2	169.2	5MSZ
CopC*	$P2_12_12_1$	A	2.03	2.06	1.97*	2.30*	N/A	2.37	91.5	(79.1)*	(170.3)*	5ICU
*Nc*AA9F#	$P2_12_12_1$	B	2.12	1.96	1.98	2.16#	2.60	2.68#	92.3	94.3	172.2	4QI8

¤ Θ1: NH_2-Cu-Nδ; Θ2: NH_2-Cu-Nε; Θ3 Nδ-Cu-Nε.

§ Tyr occupy this position in *Td*AA15 and *Nc*AA9F. *La*X325 does not have an equivalent Tyr, but the Asp122 side chain oxygen not providing equatorial coordination is found at a 2.94±0.09 Å distance to the Cu (distorted compared to octahedral coordination).

* in CopC, these equatorial ligands are swapped compared to the other Cu sites, and the Cu is coordinated by Nδ rather than Nε (Consequently, for CopC the angles are defined as Θ2: NH_2-Cu-O and Θ3: Nδ-Cu-O).

Asp33 from a symmetry-related molecule occupy these ligand positions with distorted geometry

Supplementary Table 4: EPR spin Hamiltonian parameters from simulations of cw X band spectra. *La*X325 was analysed in 50 mM Na acetate buffer pH 5.2.

		*La*X325
g values	g_x	2.040
	g_y	2.076
	g_z	2.260
A_{Cu} (MHz)	$\|A_x\|$	42
	$\|A_y\|$	64
	$\|A_z\|$	543
SHF A_N (principal values) (MHz)		28, 32, 36
A_{cu} strains (MHz)		46, 80, 80
Line widths		0.5, 0.4
Frequency (GHz)		9.315043

Supplementary Table 5. X325 encoding genes upregulated in some symbotic fungi. Cenge = *Cenococcum geophilum*, Tubma = *Tuber magnatum*, Oidma = *Oidiodendron maius*, Melbi = *Meliniomyces bicolor*, Rhier = *Rhizoscyphus ericaceae*. FLM: free-living mycelium; ECM: ectomycorrhizal; FC: fold change; FDR: false discovery rate. Each expression represents the mean of triplicate values. *Students't-test: values were calculated by comparing relative quantification measured in ECM with that in FLM.

Ectomycorrhizae				
X325 encoding genes	**FLM mean expression**	**ECM mean expression**	**FC ECM vs FLM**	**FDR *p*-value***
Cenge 644941	185	412	2.2	6.27E-06
Tubma 360409	5	474	91.5	3.83E-01
***Lb*X325**	**56**	**354**	**11.3**	**1.20E-09**
Ericoid mycorrhizae				
Oidma 153540	64	250	3.9	3.44E-21
Melbi 531740	29	108	3.8	2.72E-04
Rhier 571157	26	440	16.9	5.15E-07
Rhier 645372	1	22	16.1	1.38E-06

Supplementary Table 6. Statistical parameters of Kolmogorov-Smirnov tests performed on the immunogold labelling data (Supplementary Figure 8). FLM, free living mycelia; ECM, ectomycorrhiza.

	FLM		ECM	
	WGA	*Lb*X325	WGA	*Lb*X325
min	-0.598	-0.752	-1.957	-1.207
Q1	-0.218	-0.002	-0.183	-0.057
med	-0.035	0.311	0.016	0.188
Q3	0.214	0.536	0.267	0.494
max	1.457	1.371	2.509	2.013
n	161	161	161	161

Supplementary Figures

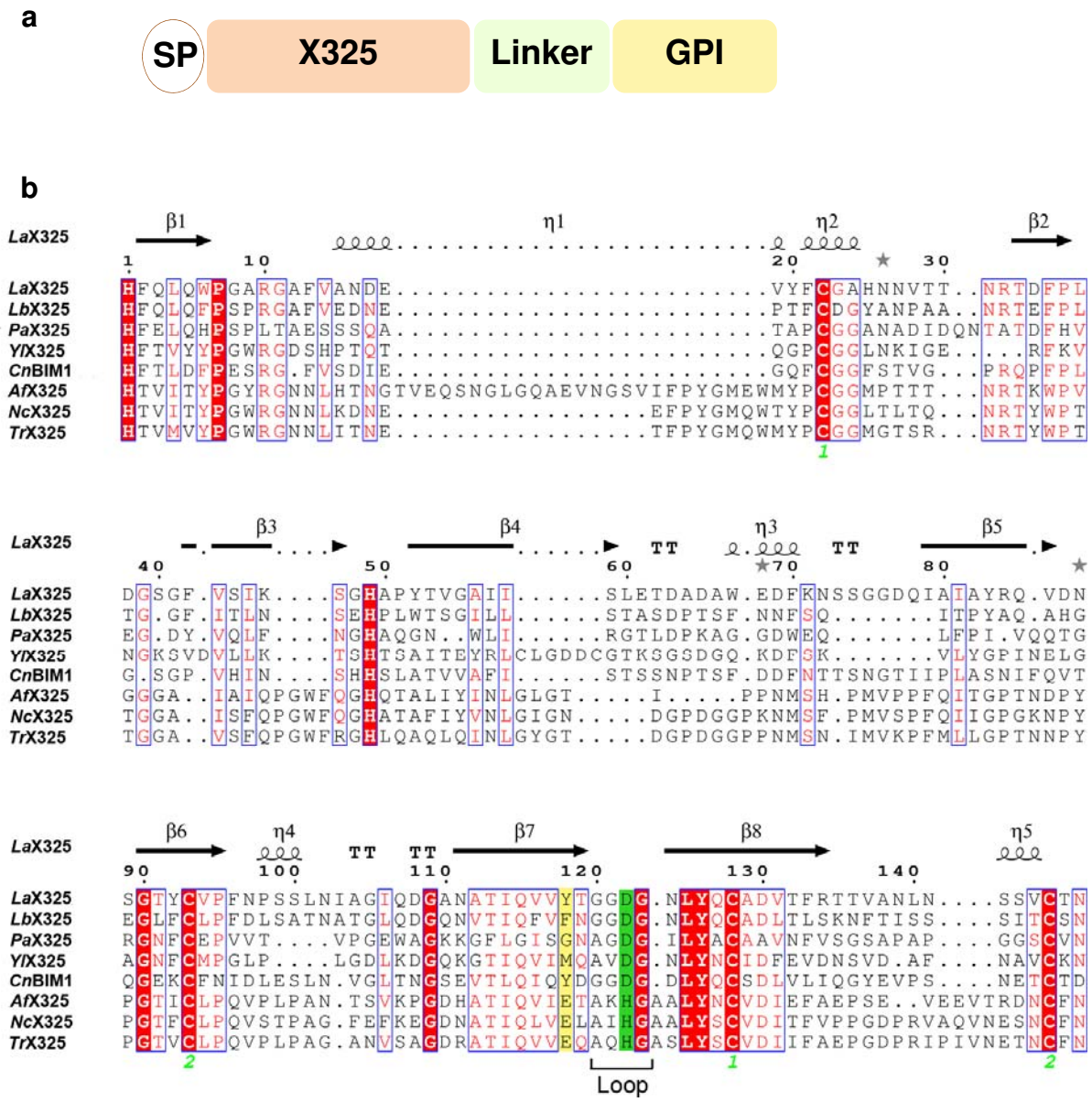

Supplementary Figure 1. Modularity (a) and structure-based sequence alignment (b) of family X325.

(a) In the N-terminal region, the signal peptide (SP) is followed by the X325 catalytic module. A linker separates the catalytic module and the C-terminal glycosylphosphatidylinositol (GPI) anchor. **(b)** The catalytic module of *La*X325 is compared with some others X325 members. The helices and strands are represented as *helices* and *arrows*, respectively, and turns are marked with *TT*. This sequence alignment was created using the sequences coming from the following organisms: *La*X325 (*Laetisaria arvalis,* MK088083, residues 1–147), *Lb*X325 (*Laccaria bicolor,* GenBank ID XM_001874260.1, residues 1–139), *Pa*X325 (*Podospora anserina,* GenBank ID XM_001907524.1, residues 1–135), *Yl*X325 (*Yarrowia lipolytica,* GenBank ID XM_505821.1, residues 1–140), *Cn*BIM1 (*Cryptococcus neoformans* X325,

GenBank ID XM_569628.2, residues 1–144), *Af*X325 (*Aspergillus fumigatus,* GenBank ID KEY79179.1, residues 1–173), *Nc*X325 (*Neurospora crassa,* GenBank ID XM_011394541.1, residues 1–163), and *Tr*X325 (*Trichoderma reesei,* GenBank ID XM_006963964.1, residues 1–163). *Dark shaded boxes* enclose invariant positions, and *light shaded boxes* highlight positions with similar residues. *Green numbers* highlight the cysteines involved in disulfide bonds. The *yellow* highlights the position of the Tyr118 in *La*X325 structure, which is not conserved across the X325 family. The *green* highlights the position of the Asp122 in *La*X325 structure. The figure was created with ESPript (http://espript.ibcp.fr).

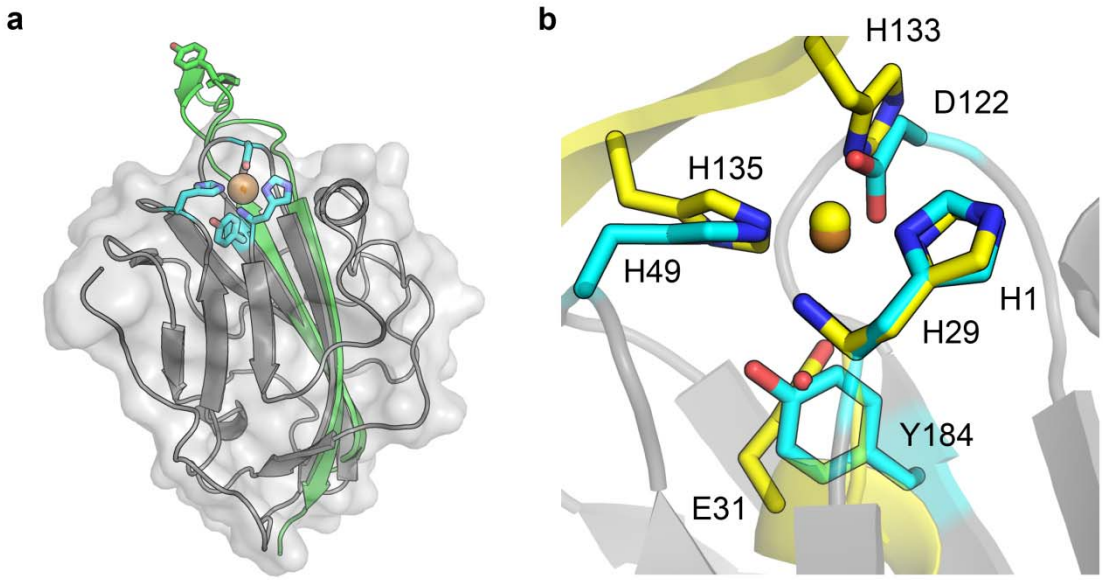

Supplementary Figure 2. Structure comparison of *La*X325 to *Td*AA15A and the Cu_B copper center of particulate methane monooxygenases (pMMOs).
(a) Superimposition of *Td*AA15 (*green*) onto *La*X325 (*grey*). Of the *La*X325 active site residues (*cyan*), Asp122 is found on a short loop equivalent to the AA15 extended protruding loop bearing a conserved Tyr (*green*). **(b)** Superimposition of copper binding sites of *La*X325 (*cyan* and *copper*) and the Cu_B center of pMMO from *Methylocystis sp.* strain M (*yellow*, Chain I of PDB entry 3RFR). A subgroup of X325 displays a His instead of Asp (Asp122 in *La*X325) in one of the equatorial Cu-coordinating ligand positions, and in addition a Glu instead of the Tyr near the active site copper (Tyr184 in *La*X325), which bears some resemblance to pMMOs.

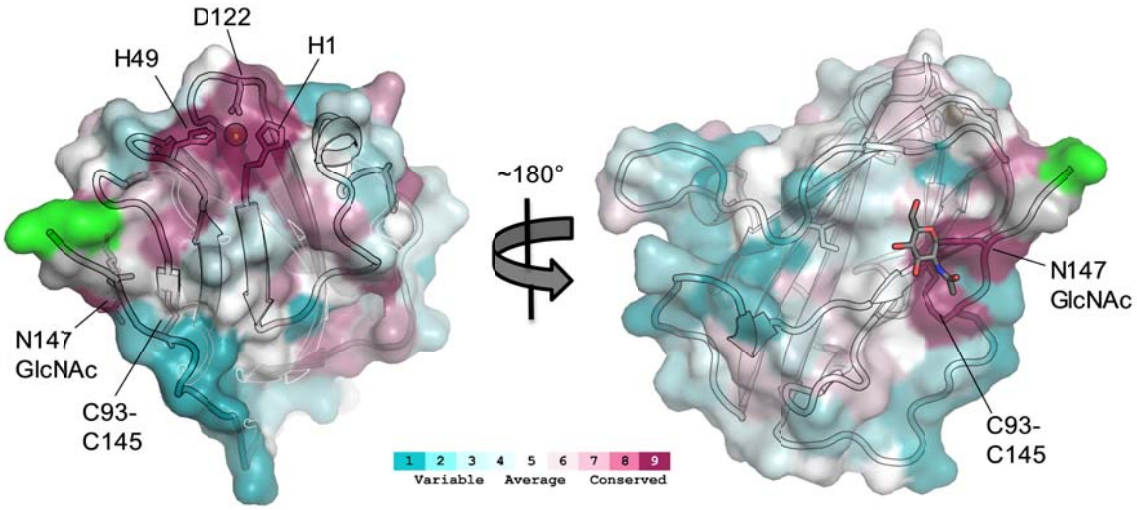

Supplementary Figure 3. Sequence conservation mapped onto the *La*X325 structure.
The *La*X325 structure (PDB 6IBJ) is shown with surface color according to sequence conservation within the X325 protein family using the 123 sequences used to build the phylogenetic tree (**Figure 1**). Conserved regions are shown in magenta and variable regions in cyan. The Cu-coordinating residues His1, His49 and Asp122 are highly conserved (left). A second conserved patch is found near the C-terminus (green) formed by a disulfide bond (Cys93-Cys145) and Asn145 (involved in N-linked glycosylation). The figure was prepared using ConSurf (http://consurf.tau.ac.il/2016/credits.php).

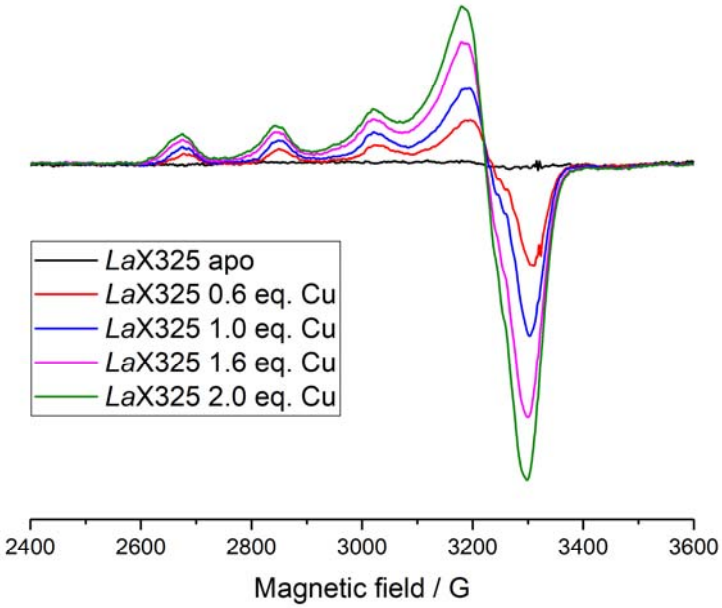

Supplementary Figure 4. Continuous wave X-band EPR Cu titration spectra (~9.3 GHz, 165 K) of *La*X325. For clarity, only a selection of spectra is presented; full data are available through the Research Data York (DOI: 10.15124/a034974e-2782-415e-8b02-2b6e4098760e)

a

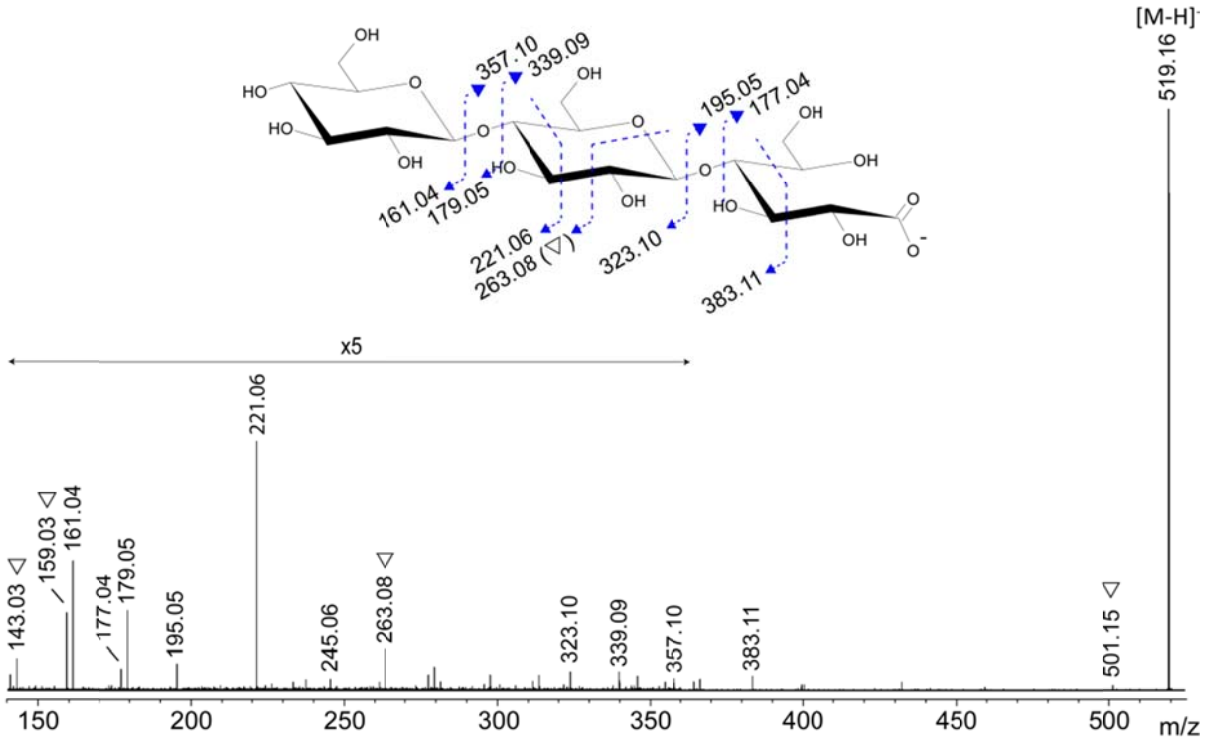
[M-H]-
519.16
357.10
339.09
195.05
177.04
161.04
179.05
221.06
263.08 (▽)
323.10
383.11
x5
143.03 ◁
159.03 ◁
161.04
177.04
179.05
195.05
221.06
245.06
263.08 ◁
323.10
339.09
357.10
383.11
501.15 ◁
150
200
250
300
350
400
450
500
m/z

b

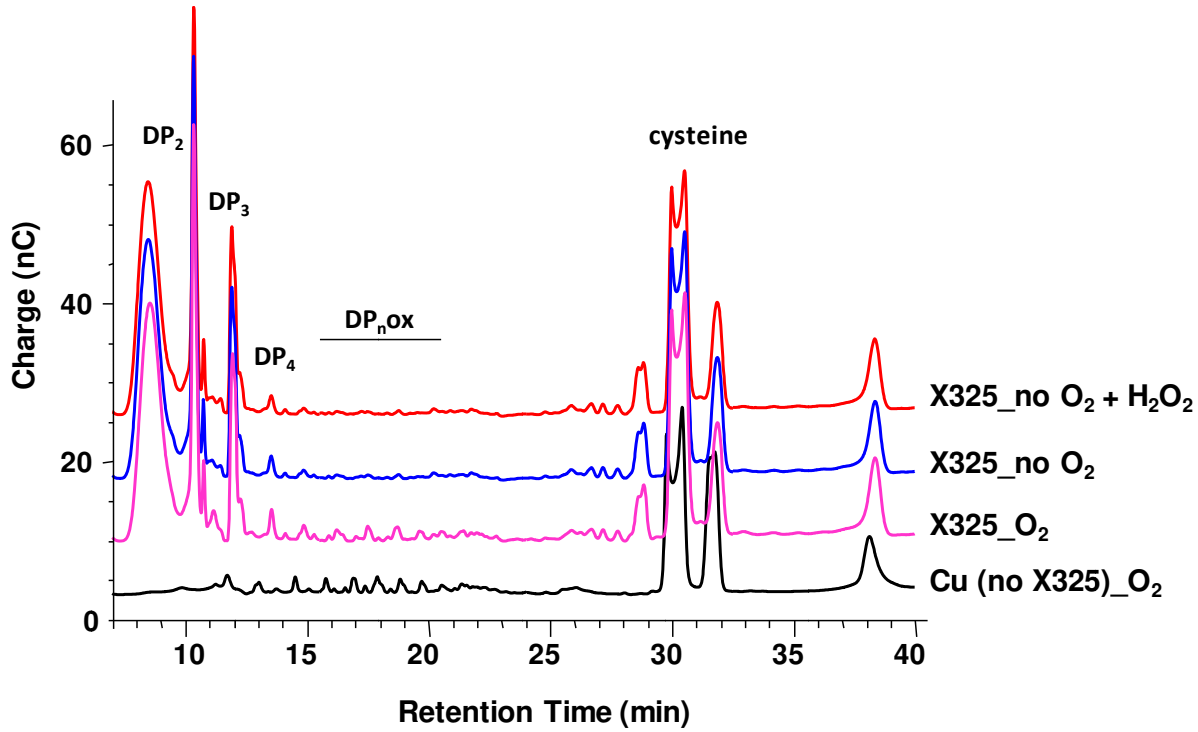
DP2
DP3
DP4
DPnox
cysteine
Charge (nC)
Retention Time (min)
X325_no O2 + H2O2
X325_no O2
X325_O2
Cu (no X325)_O2

c

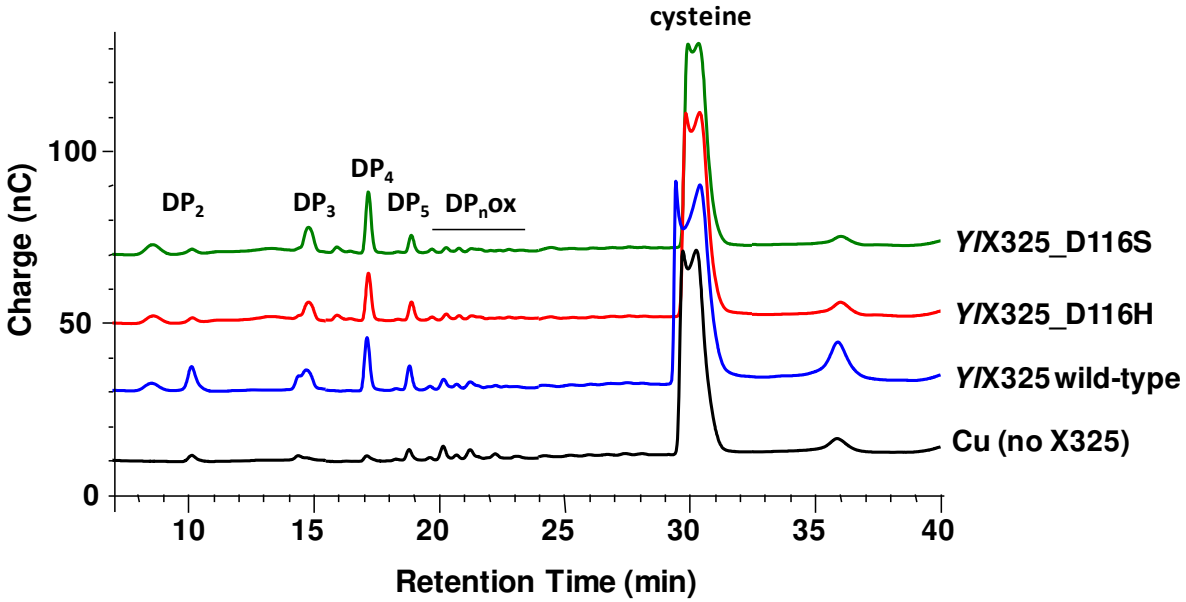

Supplementary Figure 5. Detection of soluble products generated by the action of X325 proteins on cellulose. (a) MS/MS identification of the G3 oxidized species detected at 519.16 *m/z* generated from Avicel by *La*X325. The fragmentation pattern corresponds to a C1 oxidized species with an aldonic acid at the reducing end. The structure represents a C1 oxidized cellotriose deduced from the spectrum. ▽: water losses. (**b**) Polysaccharides cleavage assays under anaerobic conditions. Reactions were carried out as described in material and methods using 5 µM X325 proteins or $CuSO_4$ with and without O_2. Addition of 50 µM of H_2O_2 was also attempted under anaerobic conditions. Chromatograms are representative of triplicate independent experiments. Peaks were assigned according to standards. **(c)** Polysaccharides cleavage assays following mutagenesis of the Asp116 residue of *Yl*X325 (equivalent to Asp122 in *La*X325) to either Ser (D116S) or His (D116H). Reactions were carried out as described in material and methods using 1 µM X325 wild type or mutant proteins or $CuSO_4$. Chromatograms are representative of triplicate independent experiments. Peaks were assigned according to standards.

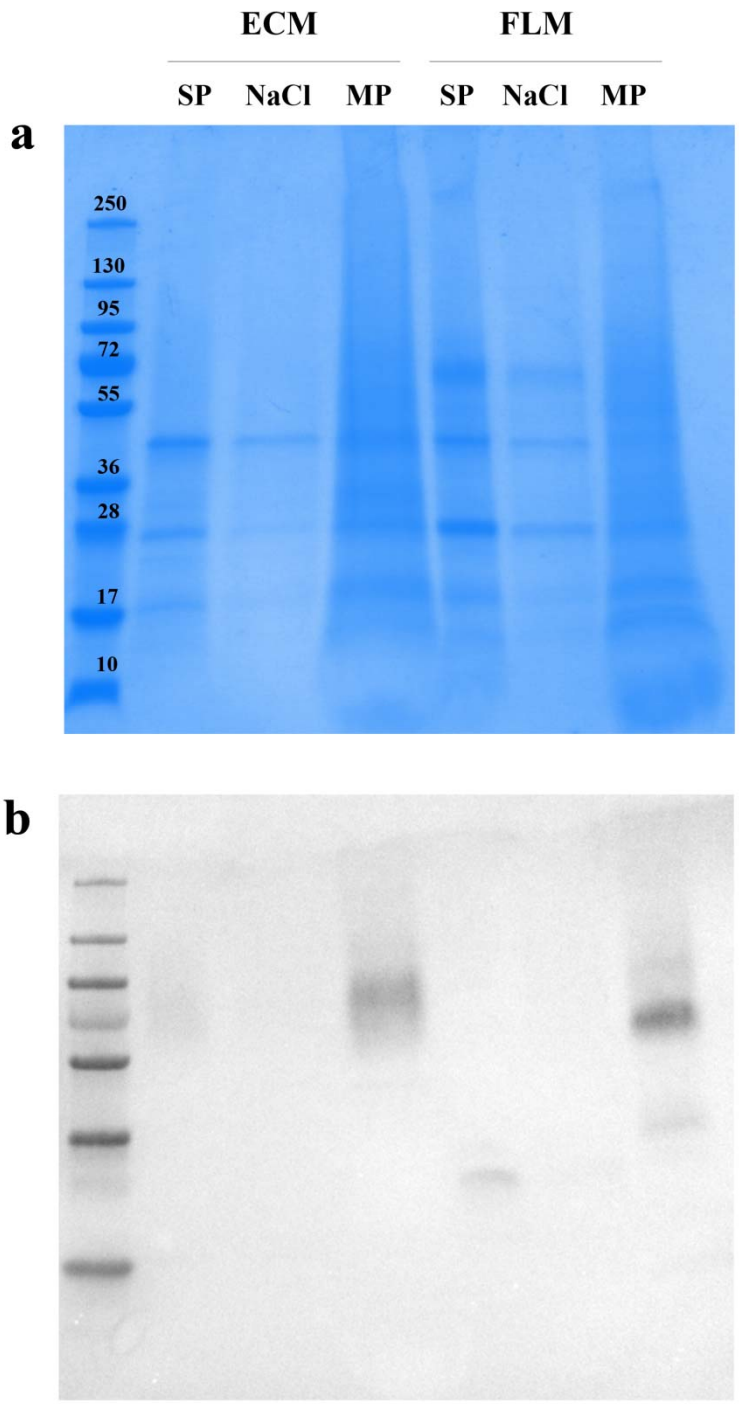

Supplementary Figure 6. Protein electrophoresis of *L. bicolor* S238N crude extracts (a) and the corresponding western immunoblotting using antibodies raised against the purified recombinant *Lb*X325 (b). Data were acquired from a single experiment. ECM = ectomycorrhizal roots, FLM = free living mycelia, SP = soluble protein fraction, NaCl fraction = proteins not covalently bound, MP = proteins attached to the membrane. For both gels, 20 µl of each crude extract fractions were loaded. Protein Ladder Range is indicated in kDa. See materials and methods.

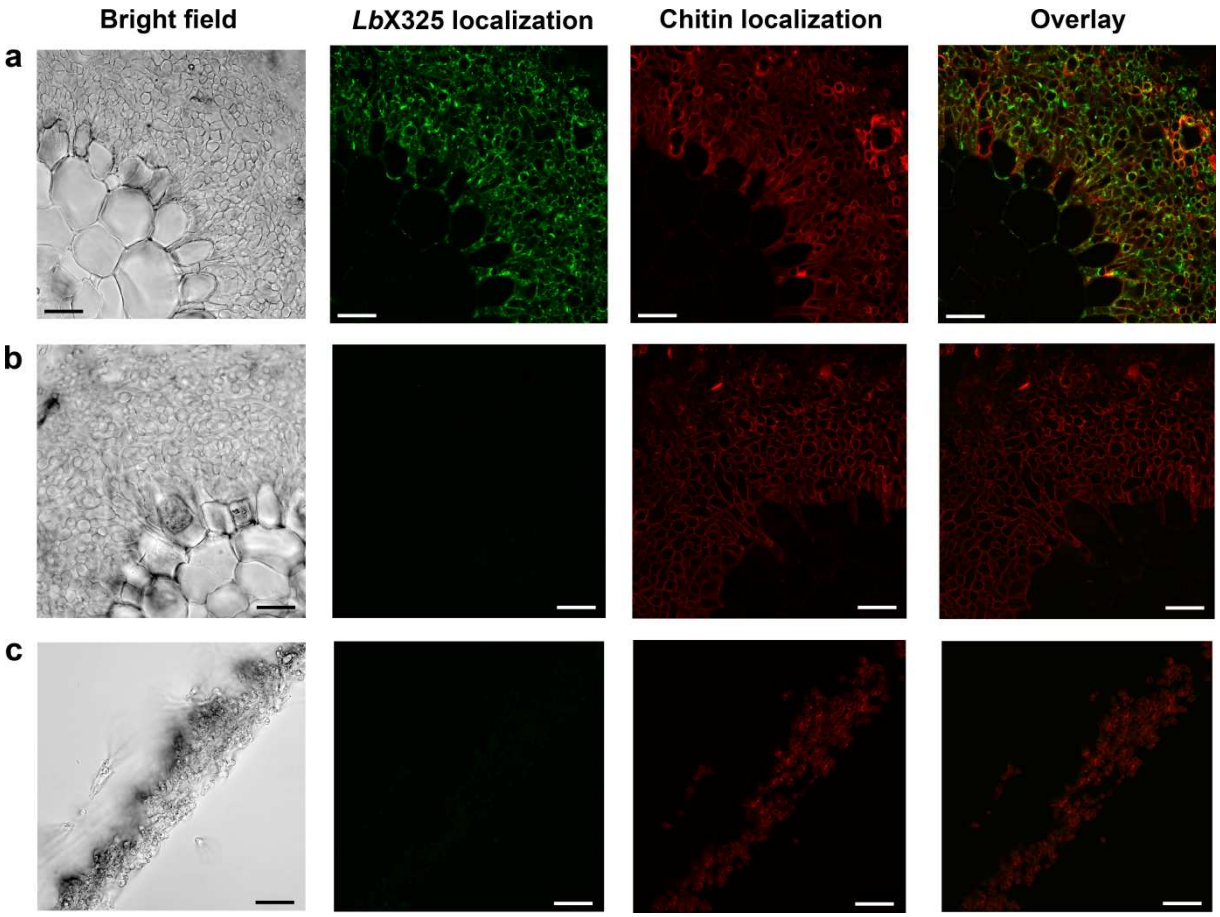

Supplementary Figure 7. Immunolocalization of *Lb*X325 in *Populus*– *Laccaria bicolor* ectomycorrhiza. All images were obtained by using indirect immunofluorescence confocal laser microscopy, except the bright field images. (**a**) Transverse sections of 3-weeks-old ectomycorrhiza stained for *Lb*X325 with anti-*Lb*X325 immune serum (green) and for chitin with wheat germ agglutinin (WGA) (red). (**b**) Binding of the anti-*Lb*X325 antibodies was blocked by incubating the sections with recombinant *Lb*X325 protein, confirming the specificity of the immune serum. (**c**) Sections of *L. bicolor* free-living mycelium stained for *Lb*X325 with anti-*Lb*X325 immune serum (green) and for chitin with WGA (red). Bars = 20 µm. Selected images are representative of five different sections.

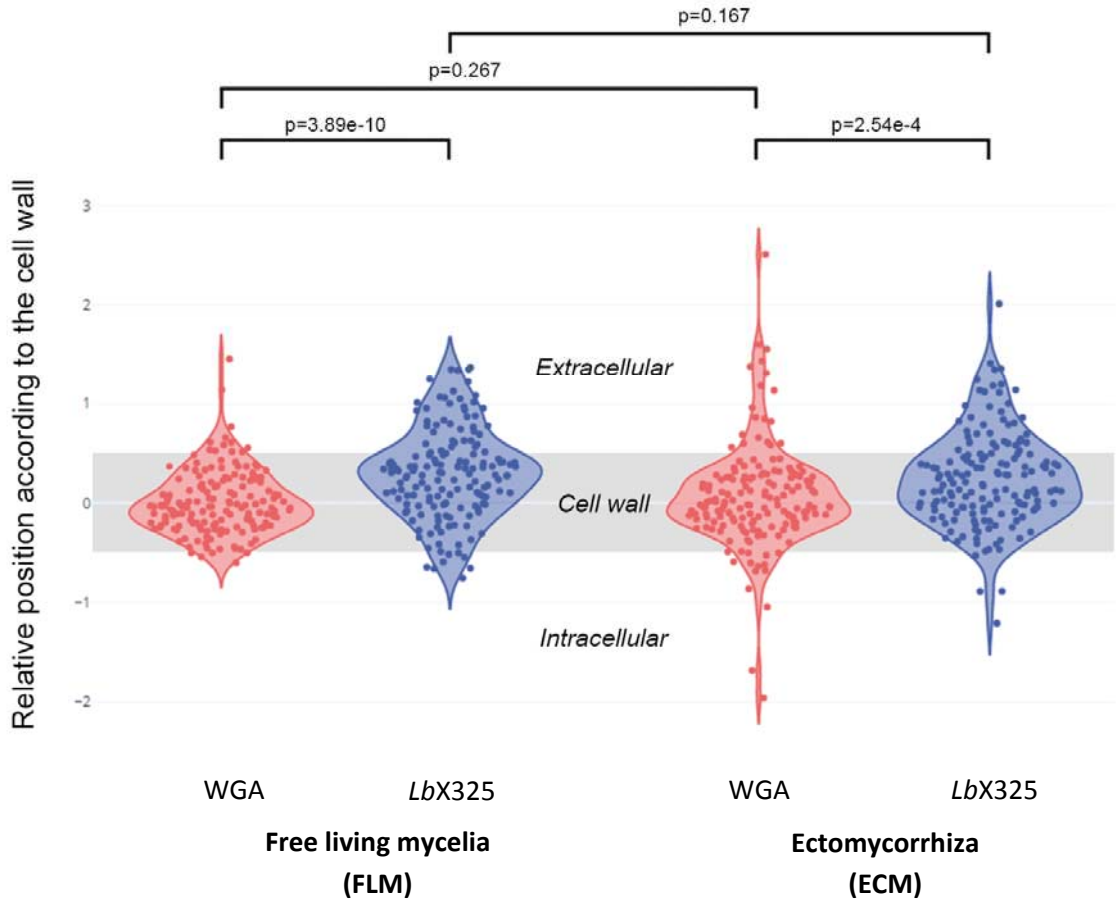

Supplementary Figure 8. Quantitative approach of immunogold labelling on transverse sections of 3-weeks-old free living mycelia (FLM, left) and ectomycorrhiza (ECM, right) indicates a preferential localization of *Lb*X325 within and beyond the outer layers of the cell wall. The Wheat Germ Agglutinin (WGA) staining is used as a control for the fungal cell wall position (chitin). As expected, the relative position of the WGA staining coincide with the cell wall position defined by morphological analysis (grey area, after normalization, between positions -0.5 and +0.5, see material and methods). The WGA staining shows no significant difference in its relative position according to the cell wall center between the FLM and ECM conditions. In both FLM and ECM conditions, the *Lb*X325 staining shows a significant shift towards the outer layers of the cell wall. The statistical analysis was done carrying out Kolmogorov-Smirnov tests (n=161 beads for each staining within each condition). The test was two-sided. Statistical parameters are listed in **Supplementary Table 6**.

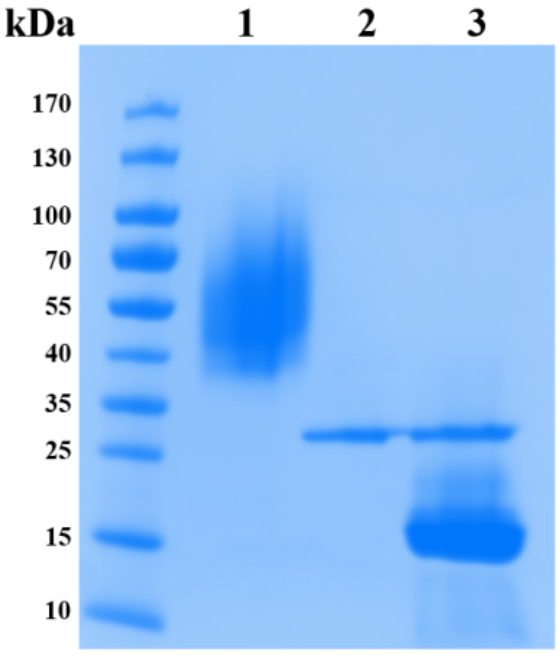

Supplementary Figure 9. SDS-PAGE analysis of *La*X325 control samples (lane 1), control endoH (lane 2) and endoH-deglycosylated *La*X325 sample (lanes 3) as described in materials and methods. 20 µg of *La*X325 protein was loaded onto the gel. Data were acquired from a single experiment.